CSMA 2024
16ème Colloque National en Calcul des Structures
13-17 Mai 2024, Presqu'île de Giens (Var)

Iterative fluid-structure resolution, correlation on a simplified composite blade tested in a traction canal

Q. Rakotomalala[1,2], C. Leblond[1], G. Dolo[1],
A. Ducoin[3], L. Rouleau[2], J-F. Deü[2]

[1] *CESMAN, Naval Group, {quentin.rakotomalala, cedric.leblond, guillaume.dolo}@naval-group.com*
[2] *LMSSC, CNAM Paris, {jean-francois.deu, lucie.rouleau, quentin.rakotomalala.auditeur}@lecnam.net*
[3] *LHEAA, Ecole Central Nantes, antoine.ducoin@ec-nantes.fr*

Résumé — In this paper, a simple coupling algorithm is used to solve the fluid-structure interaction of composite blades in water. The coupling algorithm calls in an iterative fashion black-box structural and fluid solvers. The algorithm is tested on full carbon-epoxy blade (monolithic blade) and a carbon-epoxy blade embedded with a visco-elastic layer (sandwich blade). The numerical procedure's results were compared with success to experimental data acquired at Ecole Centrale Nantes.
Mots clés — fluid structure interaction, composite, hyper-elastic layer, finite element method, lifting line

1 Introduction

Marine propellers with composite blades have many advantages. First the low density of carbon or glass fabrics combined with their high elastic modulus allow to build much lighter blades. Also, as they can be build by a layup of individuals plies, extra materials (like dampening visco-elastic layers) can be embedded at a chosen position in the blade. Finally, these blades suffer high displacement when generating thrust. These displacements can be used to optimize the shape of the blade on different operating points [1].

As the blades suffer high displacements, the fully coupled fluid-structure equation must be solved. Moreover, the pre-stress and pre-strain can have a non negligible impact on the damping characteristics of the visco-elastic layers and therefore on the blade vibration response. In this paper, a simple iterative coupling algorithm for the resolution of static fluid-structure interaction of lifting surfaces proposed in [2] is applied to a simplified blade. The numerical results are compared to experimental data that were acquired in Ecole Centrale Nantes towing tank. The blades are instrumented with optic fiber Bragg grating and a six axes hydrodynamic balance. Comparison can be carried out on both the local deformation and the global lift and drag of the blade.

2 Description of the composite blades

The simplified marine propeller blade geometry is a one meter long foil with NACA 0006 sections. The chord varies linearly along the spar and is 250 mm long at the root and 75 mm long at the tip. Two different pre-preg carbon/epoxy fabrics were used : a unidirectional fabric (UD) and a woven fabric. Figure 1a shows the layup of the blade. On the central symmetric pattern is made of 5 UD plies and 2 outer woven plies. On both side of the central pattern, a macro-ply made of 4 UD and 1 woven is repeated until there is no space left.

Two blades were build and tested, a so called *sandwich blade* which has an embedded visco-elastic layer in the central ply and a so called *monolithic blade* that is made of pure carbon-epoxy. Figure 1b shows the geometry and position of visco-elasic layer in the central layer, its parameters are : ($l_{\text{ROOT}} = 50$ mm, $L = 600$ mm, $\Delta_{le} = 15$ mm, $\Delta_{te} = 25$ mm). The two composite fabrics are modeled by an orthotrope Saint-Venant-Kirchhoff constitutive law. The visco-elastic layer is modeled using a Mooney-Rivlin hyper-elastic constitutive law. Table 1 show the approximate moduli of the composite fabrics and the moduli of the visco-elastic layer.

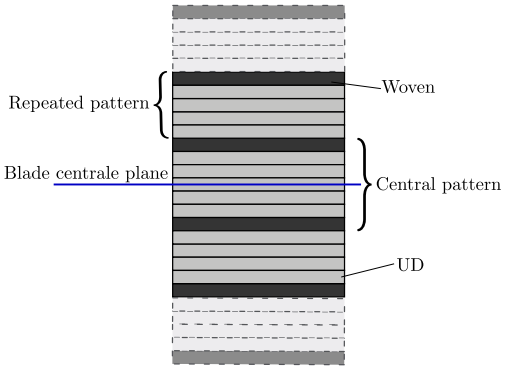

(a) Theoretical layup of the blade

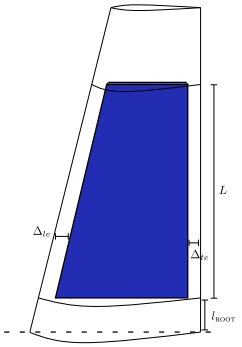

(b) Position of the visco-elastic patch

FIGURE 1 – Details of the composite layup

Composite										
fabric	E_1	E_2	E_3	G_{12}	G_{23}	G_{13}	ν_{12}	ν_{23}	ν_{13}	ρ_s
UD	165 GPa	8 GPa	8 GPa	5 GPa	4 GPa	4 GPa	0.4	0.01	0.01	1500 kg.m^{-3}
Woven	65 GPa	65 GPa	10 GPa	5 GPa	3 GPa	3 GPa	0.01	0.2	0.2	1500 kg.m^{-3}
Visco-elastic										
C_1			C_2			K			ρ	
0.53 GPa			0.24 GPa			2.1 GPa			1400	

TABLE 1 – Approximate fabrics properties.

3 Numerical resolution

The composite blade is expected to suffer large displacement, therefore the coupling between the flexible blade and the lifting fluide must be taken into account. The fluid-structure interaction problem is considered stationary and the non-linear set of equations read :

$$\begin{cases} \rho(\boldsymbol{v}\cdot\nabla)\boldsymbol{v} &= -\nabla p & \text{in } \Omega^f \\ \nabla\cdot\boldsymbol{v} &= 0 & \text{in } \Omega^f \\ \nabla_1\cdot\boldsymbol{\sigma} &= 0 & \text{in } \Omega^s \\ \boldsymbol{\sigma}\boldsymbol{n} &= -p\boldsymbol{n}_1 & \text{on } \partial\Omega^s \\ 0 &= \langle \boldsymbol{v},\boldsymbol{n}\rangle & \text{on } \partial\Omega^s \\ \lim_{|\boldsymbol{x}|\to\infty}\boldsymbol{v} &= \boldsymbol{v}_\infty & \end{cases} \tag{1}$$

where $\boldsymbol{v}$ is the fluid velocity, $\boldsymbol{u}$ the structural displacement, p the fluid pressure and $\boldsymbol{n}$ the normal of the blade's wetted area. Symbolically, Equation 1 can be rewritten :

$$\begin{cases} p &= \mathcal{F}(\boldsymbol{u}) \\ \boldsymbol{u} &= \mathcal{S}(p) \end{cases} \tag{2}$$

where $\mathcal{F}$ is the fluid solver and $\mathcal{S}$ is the structural solver. This coupled system of equation was solved using the Neumann-Neumann coupling algorithm described in [2]. The variables $\boldsymbol{u}, p$ are approached by a sequence $(\boldsymbol{u}_1^k, p_1^k)$ defined by : $\boldsymbol{u}_1^0 = 0$, $(\boldsymbol{u}_1^k, p_1^k) = (\mathcal{S}(p_1^k), \mathcal{F}(\boldsymbol{u}_1^{k-1}))$. In this paper, the structural solver uses non linear *Finite Element Method*(FEM) through the software code_aster [3] and the fluid solver is a lifting line method.

This simplified method computes the pressure field generated by a 3D foil. The foil is sliced into infinitesimal section, the Joukowski theorem applied to a section r states that the infinitesimal section can be modeled by a vortex filament with circulation $\Gamma(r)$, with $\Gamma(r) = C_l(\alpha^{\text{EFF}}, v^{\text{EFF}})v^{\text{EFF}}c(r)$ where α^{EFF} and v^{EFF} are the local incident flow on section r. As the circulation must be constant along a vortex filament each variation of Γ creates a horseshoe vortex of circulation $\partial_r\Gamma(r)$ which is convected in the flow. These horseshoe vortices create a wake velocity field that locally modifies the incident flow $(\alpha^{\text{EFF}}, v^{\text{EFF}})$, the vorticity distribution $\Gamma(r)$ is therefore determined by solving a non linear integro-differential equation.

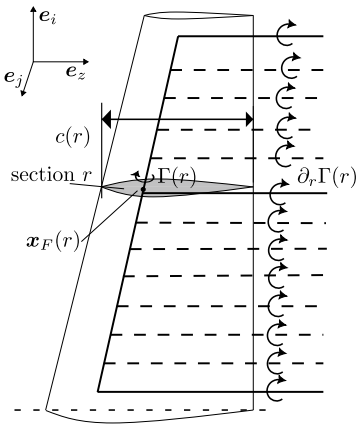

FIGURE 2 – Lifting line principle

Once $\Gamma(r)$ is determined, the pressure field can be computed on each sections and extrapolated on the whole blade. The method gives the local lift per section $\delta L(r)$ and an induced drag coefficient $\delta D^{\text{IND}}(r)$. A viscous contribution can be added to the drag using the friction boundary layer law $\delta D(r) = \delta D^{\text{IND}}(r) + 0.5\rho(v^{\text{EFF}}(r))^2\delta S(r)\frac{0.455}{\log_{10}(\text{Re})^{2.58}}$ where $\delta S(r)$ is the surface of the infinitesimal section r and Re is the Reynold number based on the chord at section r. The global lift coefficient $C_l = \int \delta L(r)/(1/2\rho v_\infty^2 S)$ and drag $C_d = \int \delta D(r)/(1/2\rho v_\infty^2 S)$ can therefore be computed.

4 Description of the experimental setup

The composite blades were instrumented with optic fiber Bragg grating, as displayed on figure 3a, the 16 sensors are distributed on two optic fiber embedded on the surface of the blade. Each optic fiber makes a loop in the layup and both ends can be used for measurements, this setup is more resilient as if the fiber breaks the sensors can still be used from one of the ends of the optic fiber. Hydrodynamic quantities (lift, drag, weight and associated moments) are measured using a 6 axes hydrodynamic balance (see Figure 3b).

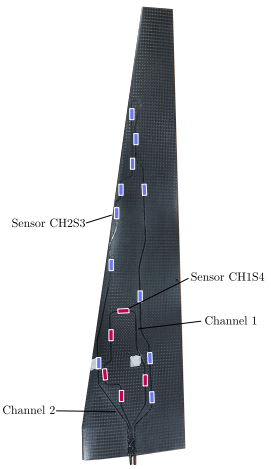

(a) Blade instrumented with optic fibers

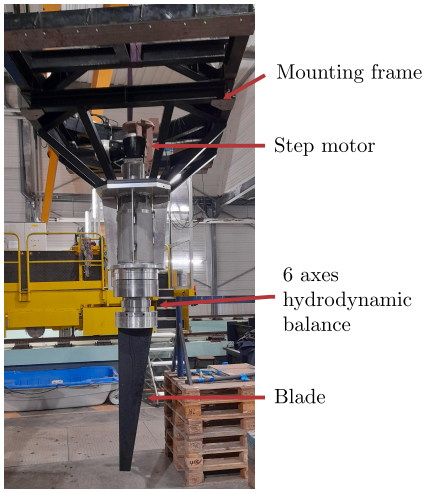

(b) Blade mounted on the towing tank support with the hydrodynamic balance and step motor

FIGURE 3 – Instrumented blade

The blades were tested in the towing tank of Ecole Centrale Nantes. This tank is 140 meters long, 5 meters wide and has a constant depth of 3 meters. It is equipped with a towing carriage that can go up to 8 m/s (see Figure 4a), a step motor allows to control the incidence of the blade. In order to smooth as much as possible the incident flow on the blade and avoid free surface phenomena, the blade is placed

under a specially designed hull (see Figure 4b and 4a).

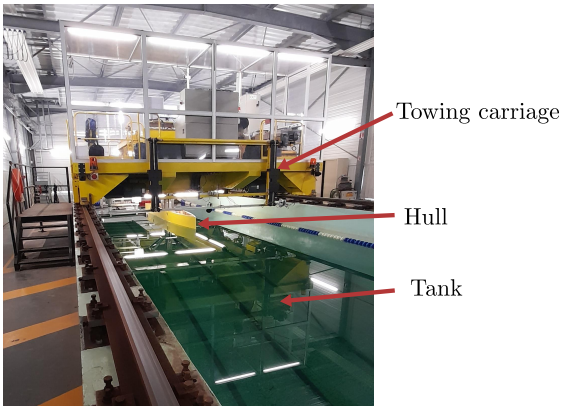

(a) Towing carriage with the instrumented blade and hull

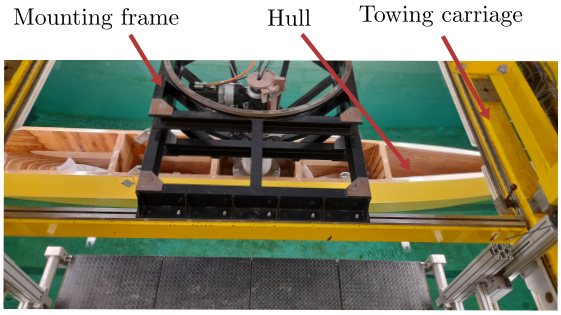

(b) Focus on the mounting frame and hull assembly

FIGURE 4 – Towing carriage

5 Experimental results and numerical computations comparison

The monolithic and sandwich blades were tested in static conditions : the angle of attack and the velocity of the chariot are constant during the whole run. The tables 2a and 2b describe the angles of attack and velocities tested. For each angle and velocity, three measurements were done.

angle \ velocity	1 m/s	3 m/s	4 m/s
0.84	✓	✓	✓
2.84	✓	✓	✓
4.84	✓	✓	✓
6.84	✓	✓	✓
9.84	✓	✓	

(a) Monolithic blade

angle \ velocity	1 m/s	3 m/s
0.35	✓	✓
2.35	✓	✓
4.35	✓	✓
6.35	✓	✓
9.35	✓	✓

(b) Sandwich blade

TABLE 2 – Descriptions of the measurement carried out

As highlighted in Figure 5a, the raw lift measurements L^{RAW} varies and contains noise. Figure 5b shows the signal filtered by a low-pass filter L^{FILT}, the static value is the temporal mean $\bar{L}^{\text{FILT}}$, and a first error of measurement is identified $\Delta L = \max L^{\text{FILT}} - \min L^{\text{FILT}}$. Another source of error comes from the fluctuation $L^{\text{RAW}} - L^{\text{FILT}}$ (see Figure 5c), Figure 5d shows that this quantity follows a Gaussian distribution and therefore an added error of $\delta L = \sigma(L)$, where $\sigma(L)$ is the standard deviation of the distribution, is considered. Therefore, for each measurement of quantity X, the error considered will be $\varepsilon(X) = \max X^{\text{FILT}} - \min X^{\text{FILT}} + \sigma(X)$

Figures 6 shows the results of the optic fibers measurements (deformation) and the 5-axes hydrodynamic balance (lift and drag) on the monolithic blade. Figures 6a,6c and 6e show that the computations and measurements are in good agreement on all the sensor considered. Figures 6b,6d and 6f shows that the lifting line reproduces the measured lift where the blade element method fails. For low angles (below 10°) the lifting line is also reproduces the drag coefficient.

Figures 7 shows the results of the optic fibers measurements (deformation) and the 5-axes hydrodynamic balance (lift and drag) on the sandwich blade. Figure 7a also shows a good agreement on all the sensors considered. Figure 7c shows that the computations give lower results than the measurement but they still give the right order of magnitude. Figures 7b and 7d show that as for the monolithic blade, the lifting line reproduces the measured lift and the drag coefficient for angles below 10°.

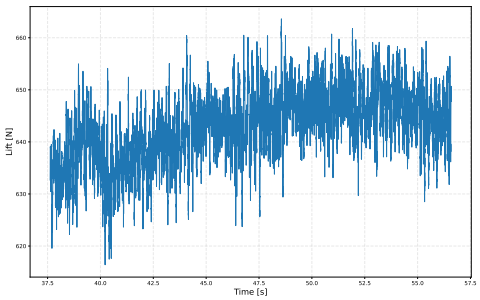

(a) Raw lift measurements

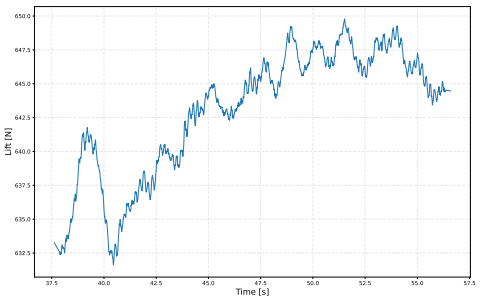

(b) Filtered lift signal

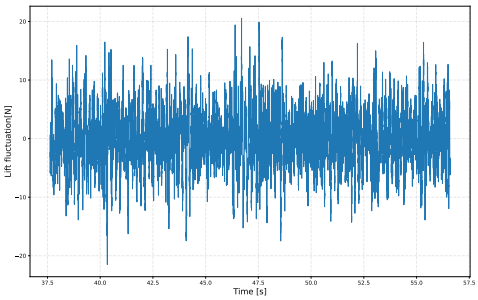

(c) Fluctuation of the lift

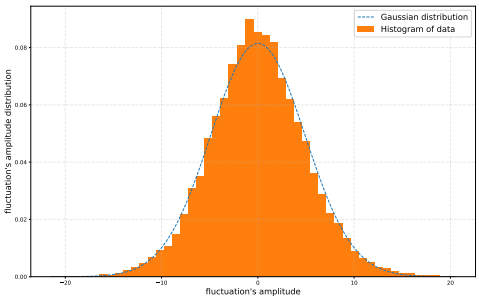

(d) Distribution of the lift fluctuation

FIGURE 5 – Exemple of raw lift measurements data on the monolithic blade for $\alpha = 6.84$ and $v = 4$ m/s

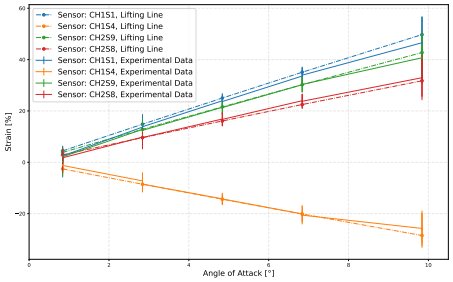

(a) Deformation 1 m/s

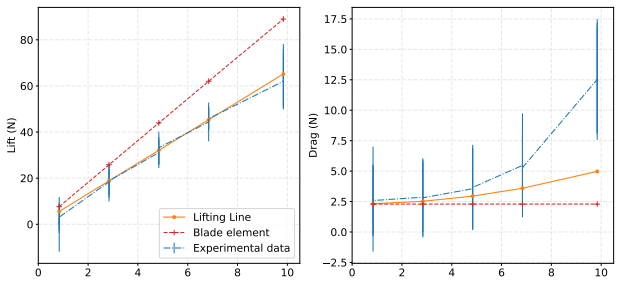

(b) Lift and Drag 1 m/s

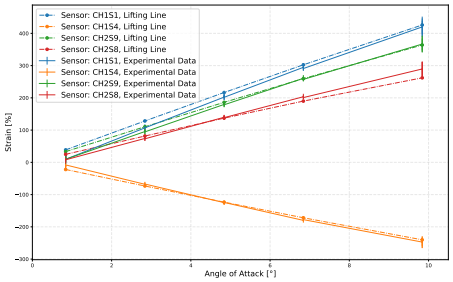

(c) Deformation 3 m/s

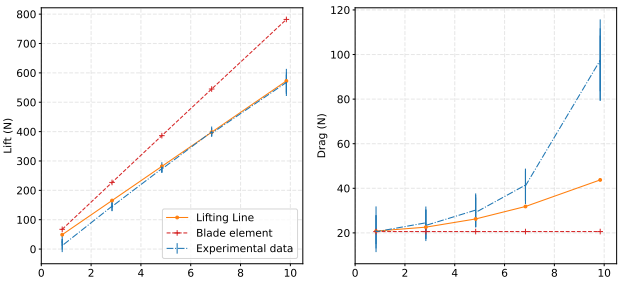

(d) Lift and Drag 3 m/s

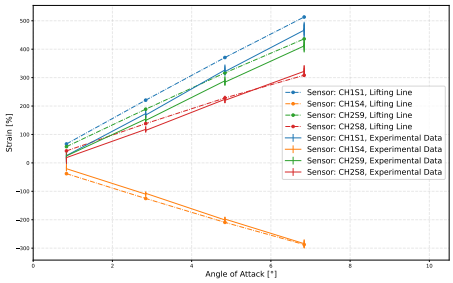

(e) Deformation 4 m/s

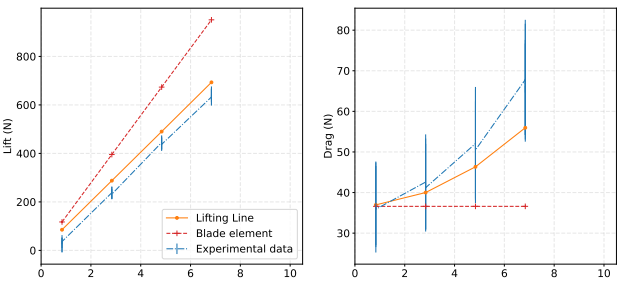

(f) Lift and Drag 4 m/s

FIGURE 6 – Comparison between the experimental results and the numerical computations on the monolithic blade

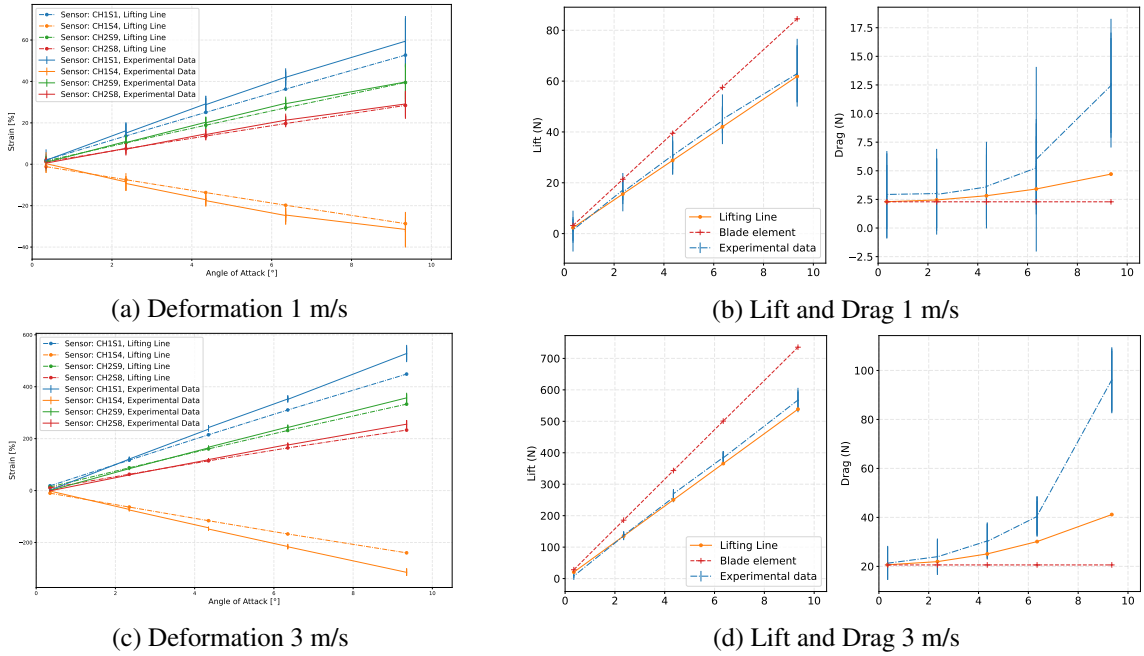

(a) Deformation 1 m/s

(b) Lift and Drag 1 m/s

(c) Deformation 3 m/s

(d) Lift and Drag 3 m/s

FIGURE 7 – Comparison between the experimental results and the numerical computations on the sandwich blade

6 Conclusions

In this paper, a simple fluid-structure iterative coupling algorithm is used to solve the interaction between a composite blade in an incident flow. The algorithm couples a finite element method structural solver with a lifting line method that allows to take into account limited 3D flow effect on the blade. These computations were compared with success to experimental data acquired in Ecole Centrale Nantes towing tank. The comparison shows that the coupling algorithm matches the lift and drag acquired with the 6 axes hydrodynamic balance and the deformation acquired with optic fibers Bragg gratings. The comparison was carried out on a monolithic blade made of only carbon-epoxy fabrics and on a sandwich blade made of the same carbon epoxy layup with a visco-elastic embedded layer.

This simple coupling algorithm could be used in the design phase to determine a layup that optimizes the hydrodynamic properties of the blade on multiple operating points. This algorithm can also be used to compute the intermediate pre-stressed configuration around which the blade vibrates, following the simplified methodology of [2].

Acknowledgment

Références

[1] Manudha T Herath, B Gangadhara Prusty, G H Yeoh, M Chowdhury, and Nigel St. Development of a shape-adaptive composite propeller using bend-twist coupling characteristics of composites.

[2] Quentin Rakotomalala, Lucie Rouleau, Cédric Leblond, Mickaël Abbas, and Jean-François Deü. A Two-Step Fluid-Structure Approach for the Vibration Analysis of Flexible Propeller Blade, May 2023.

[3] EDF. Finite element code_aster, Analysis of Structures and Thermomechanics for Studies and Research, 1989.